AGU PUBLICATIONS

Geophysical Research Letters

RESEARCH LETTER
10.1002/2014GL059647

Key Points:
- The links between European cyclones and the NAO are systematically analyzed
- NAO conditions fostering explosive/non-explosive cyclones are different
- Eddy feedback on the daily NAO index is evident for the strongest cyclones

Supporting Information:
- Readme
- Figure S1
- Figure S2

Correspondence to:
I. Gómara,
i.gomara@ucm.es

Citation:
Gómara, I., B. Rodríguez-Fonseca, P. Zurita-Gotor, and J. G. Pinto (2014), On the relation between explosive cyclones affecting Europe and the North Atlantic Oscillation, *Geophys. Res. Lett.*, *41*, 2182–2190, doi:10.1002/2014GL059647.

Received 18 FEB 2014
Accepted 26 FEB 2014
Accepted article online 3 MAR 2014
Published online 19 MAR 2014

On the relation between explosive cyclones affecting Europe and the North Atlantic Oscillation

Iñigo Gómara[1,2], Belén Rodríguez-Fonseca[1,2], Pablo Zurita-Gotor[1,2], and Joaquim G. Pinto[3,4]

[1]Dpto. Geofísica y Meteorología, Universidad Complutense de Madrid, Spain, [2]Instituto de Geociencias (IGEO), UCM, CSIC, Spain, [3]Department of Meteorology, University of Reading, UK, [4]Institute for Geophysics and Meteorology, University of Cologne, Germany

Abstract Intense winter cyclones often lead to hazardous weather over Europe. Previous studies have pointed to a link between the North Atlantic Oscillation (NAO) and strong European windstorms. However, the robustness of this relation for cyclones of varying intensities remains largely unexplored. In this paper, the bi-directional relation between the NAO and cyclones impacting Europe is analyzed for the period 1950–2010 focusing on the sensitivity to storm intensity. Evidence is given that explosive (EC) and non-explosive cyclones (NoEC) predominantly develop under different large-scale circulation conditions over the North Atlantic. Whereas NoEC evolve more frequently under negative and neutral NAO phases, the number of EC is larger under a positive NAO phase, typically characterized by an intensified jet toward Western Europe. Important differences are also found on the dynamics of NAO evolution after peak intensity for both cyclone populations.

1. Introduction

Hazardous weather conditions over Europe are frequently associated with the passage of intense extra-tropical cyclones, especially during winter [*Lamb*, 1991]. Such storms typically induce intense wind gusts and sometimes heavy precipitation and storm surges, leading to disruption of normal socio-economic activity and large property damage [e.g., *Fink et al.*, 2009]. The explosive intensification of cyclones [*Sanders and Gyakum*, 1980; pressure fall greater than 24 hPa day^{-1} at 60ºN, or equivalent], often leading to storms with hurricane-like strong winds over the eastern North Atlantic (NA), is one of the several reported sources of uncertainty in weather forecasts [e.g., *Wernli et al.*, 2002].

The anomalous mean flow over the North Atlantic on days prior, during, and after the occurrence of European windstorms has been analyzed in previous studies [e.g., *Raible*, 2007; *Pinto et al.*, 2009; *Hanley and Caballero*, 2012; *Gómara et al.*, 2013]. The North Atlantic Oscillation (NAO), the most prominent pattern influencing the European weather variability [*Hurrell et al.*, 2003], has a clear link to storm activity: under a positive NAO phase, the jet is northeastwardly shifted and accelerated over the NA, with cyclone trajectories tilted north-eastward toward northern Europe. Conversely, the negative NAO phase is characterized by a more equatorward and less eastward extended jet, with more zonal orientated cyclone tracks typically directed toward southwestern Europe [cf. *Pinto and Raible*, 2012]. As a consequence, windstorms affecting Central Europe tend to occur under a moderately positive NAO phase [*Donat et al.*, 2010], and their development can be supported by Rossby wave-breaking (RWB) processes [cf. *Hanley and Caballero*, 2012; *Gómara et al.*, 2013]. Conversely, intense cyclones themselves can also play an important role modifying the large-scale flow and thus driving the short-term NAO variability on days following their maximum intensification period [*Rivière and Orlanski*, 2007; *Michel et al.*, 2012]. However, the sensitivity of this two-way relation to cyclone's intensity has received little attention.

In this study, the bi-directional relation between the large-scale mean flow (represented by the NAO) and explosive and non-explosive cyclones affecting Western and Central Europe is examined using a long reanalysis data set. A question of prime interest is whether this relation is sensitive to storm's intensity. A daily NAO index (DNI) and three different cyclone subsets, stratified in terms of cyclone intensity, are considered.

This letter is structured as follows. Cyclone and NAO considerations are detailed in section 2. Section 3 outlines the main results, and a short discussion concludes the study.

2. Data and Methodology

The National Centers for Environmental Prediction (NCEP) reanalysis data [*Kalnay et al.*, 1996] are used over 60 extended winter seasons (October–March 1950–2010) with a 6-hourly temporal resolution and a 2.5° horizontal grid. Mean sea level pressure data (6-hourly), daily averaged geopotential height at 500 hPa (z500), and zonal and meridional winds at 250 hPa (u250, v250) are used to analyze the anomalous mean flow associated with cyclone occurrences. For each day, the monthly mean associated with the corresponding year is removed in order to compute the anomalies (e.g., if 17 March 1985 is selected, then the monthly mean of March 1985 is subtracted). This is done to remove intra-seasonal/seasonal (e.g., a more intense jet in January than in October) and long-term decadal/multidecadal variability from the anomalous fields. Finally, a 5 day (centered) running mean smoothing is applied to minimize the influence of individual cyclones onto the large-scale mean flow [cf. *Pinto et al.*, 2009]. The methods and confidence intervals used for statistical hypothesis testing (e.g., Monte Carlo, *t* test) are detailed in figure captions.

2.1. Cyclone Considerations

An automatic tracking method [*Murray and Simmonds*, 1991] adapted and validated for Northern Hemisphere cyclone characteristics [*Pinto et al.*, 2005] is applied to mean sea level pressure data to obtain complete cyclone life cycles and additional properties. Cyclone normalized deepening rate (NDR, in Bergeron) is used as indicator of intensity:

$$NDR = \frac{\Delta P}{24}\frac{\sin 60^\circ}{\sin \phi}, \quad (1)$$

where ΔP accounts for the pressure drop and Φ is the average latitude of the cyclone's surface centre over a time interval of 24 h. To ensure that cyclones affect the European continent during their mature stage, we follow *Gómara et al.* [2013] and select cyclones located within the latitude-longitude box [35°N–65°N, 20°W–10°E] (dashed rectangle in Figure 1a) at the final time step of the 24 h of maximum NDR (red segments in the 6-hourly trajectories).

Finally, depending on their maximum NDR (intensity), the selected cyclones are divided into three different subsets (Figure 1c): (1) Non-explosive cyclones (NoEC = 1665 cases; $0 < NDR_{NoEC} < 1$ Bergeron); (2) Explosive cyclones (EC = 424 cases; $NDR_{EC} \geq 1$ Bergeron); and (3) "Extreme" cyclones, defined as explosive cyclones with NDR equal or above the 95th percentile (EC95 = 104 cases; $NDR_{EC95} \geq NDR_{95th}$). Note that these are also included in (2).

Figures 1a and 1b show the complete cyclone trajectories (blue) and the segment corresponding to the 24 h maximum intensification period (red) of NoEC and EC. As a general note, it can be observed that NoEC (Figure 1a) roughly span in latitude over the entire "European box area." In contrast, EC (Figure 1b) depict more coherent and latitudinal constrained tracks over higher latitudes [50°N–65°N], as they tend to develop along an intensified jet stream [cf. *Uccellini*, 1990; *Hanley and Caballero*, 2012; *Gómara et al.*, 2013].

For the lag composite analysis, lag 0 is defined as the day in which the period of maximum NDR (24 h) starts (e.g., if a cyclone features its maximum intensification between 12 UTC 10 January and 12 UTC 11 January, then 10 January is defined as lag 0).

2.2. NAO Definition and Classification

A daily NAO index (DNI) is constructed to analyze the NAO variability at synoptic timescales [cf. *Pinto et al.*, 2009]. First, the leading EOF (Empirical Orthogonal Function) of monthly mean z500 anomalies [25°N–80°N, 80°W–40°E] over the time period October–March 1950–2010 is calculated (explained variance of 33.89%). Next, a daily index is constructed projecting the z500 daily anomalies in the Euro-Atlantic sector onto this EOF1. The resulting time series has a correlation of 0.78 with the NOAA Climate Prediction Centre (CPC) daily NAO index (99% confidence interval, bilateral *t* test). We then subtract from this time series the monthly mean DNI of the corresponding year and apply a 5 day (centered) running mean smoothing. Finally, the index is standardized. The same methodology is applied to the anomalous mean flow fields, except for the standardization.

In Figure 1d, the pattern associated with EOF1 is provided: a NAO-like structure can be identified with two centers of action, one over southern Greenland and the other spanning over the sub-tropical NA and

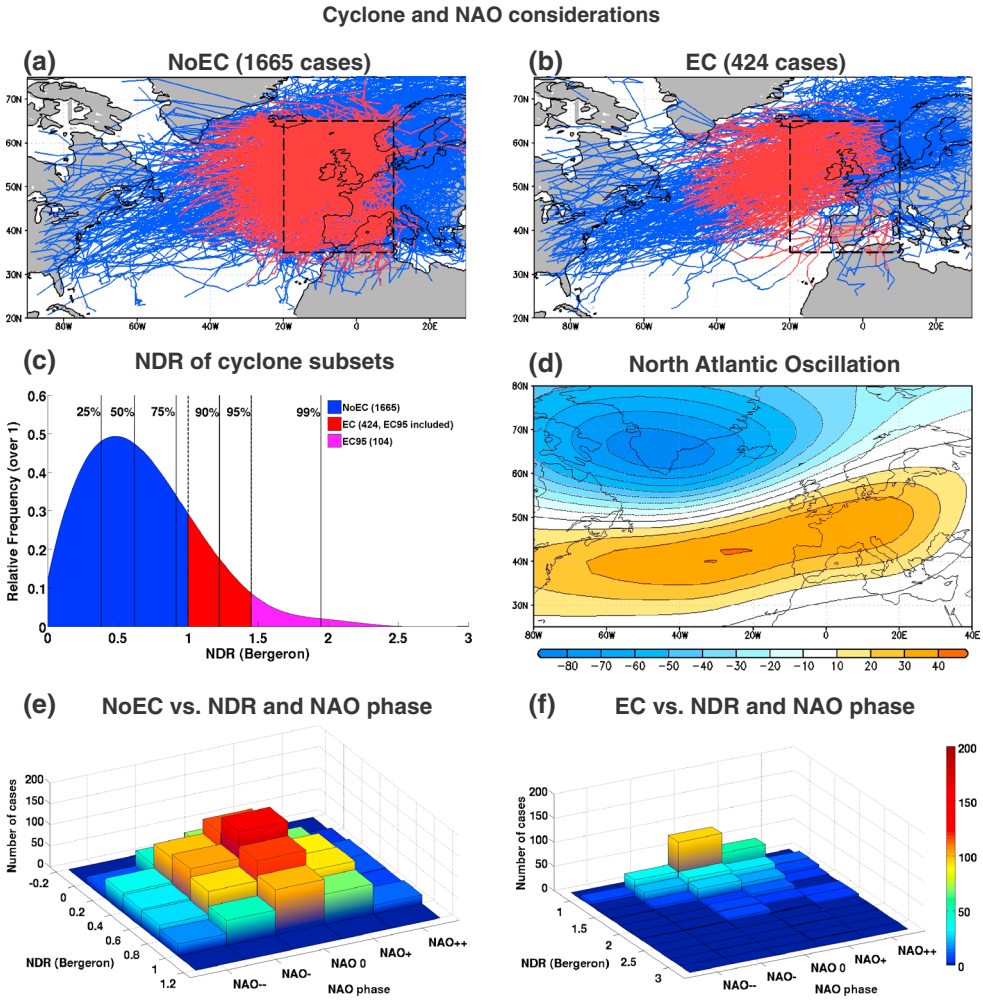

Figure 1. (a) Whole non-explosive cyclones (NoEC) trajectories (blue) and segments of maximum normalized deepening rate (NDR) (24 h, red). "European box area" for cyclone selection (dashed rectangle). (b) Same as Figure 1a but for explosive cyclones (EC). (c) Relative frequency (over 1) of cyclone NDR (curve, in Bergeron). NDR range of cyclone subsets (filled colored areas). NDR percentiles (vertical lines). (d) North Atlantic Oscillation (NAO) pattern (Empirical Orthogonal Function 1; regression map in gpm). (e) 3-D histogram of NoEC on lag 0: Number of cases vs. NDR vs. NAO phase. (f) Same as Figure 1e but for EC.

SW/central Europe. Subsequently, five different NAO phases (frequencies shown in Figure 3a, solid black line) are derived depending on the DNI value following *Pinto et al.* [2009]: NAO++ (DNI ≥ +1.5); NAO+ (+0.5 ≤ DNI < +1.5); NAO 0 (−0.5 < DNI < +0.5), NAO− (−1.5 < DNI ≤ −0.5); and NAO−− (DNI ≤ −1.5).

In Figures 1e and 1f, the 3-D histograms of cyclone counts, maximum NDR, and NAO phase (at lag 0) are provided for NoEC and EC, respectively. The total number of cyclones is highest under NAO 0 (also the most frequent phase, cf. Figure 3a). Comparing the non neutral phases, a negative NAO shift can be observed for NoEC and the reverse for EC. This asymmetry is analyzed in more detail in section 3.1.2.

3. Results

3.1. Influence of the Background Field Over the Cyclones

3.1.1. Structure of Mean Flow North Atlantic Anomalies

The anomalous mean flow over the NA on lagged cyclone days is shown in Figure 2. For EC95, a downstream propagating north-negative and south-positive pattern of z500 composite anomalies is observed (Figures 2a, 2d, and 2g). This structure resembles the positive NAO phase and is accompanied by an intensified jet stream

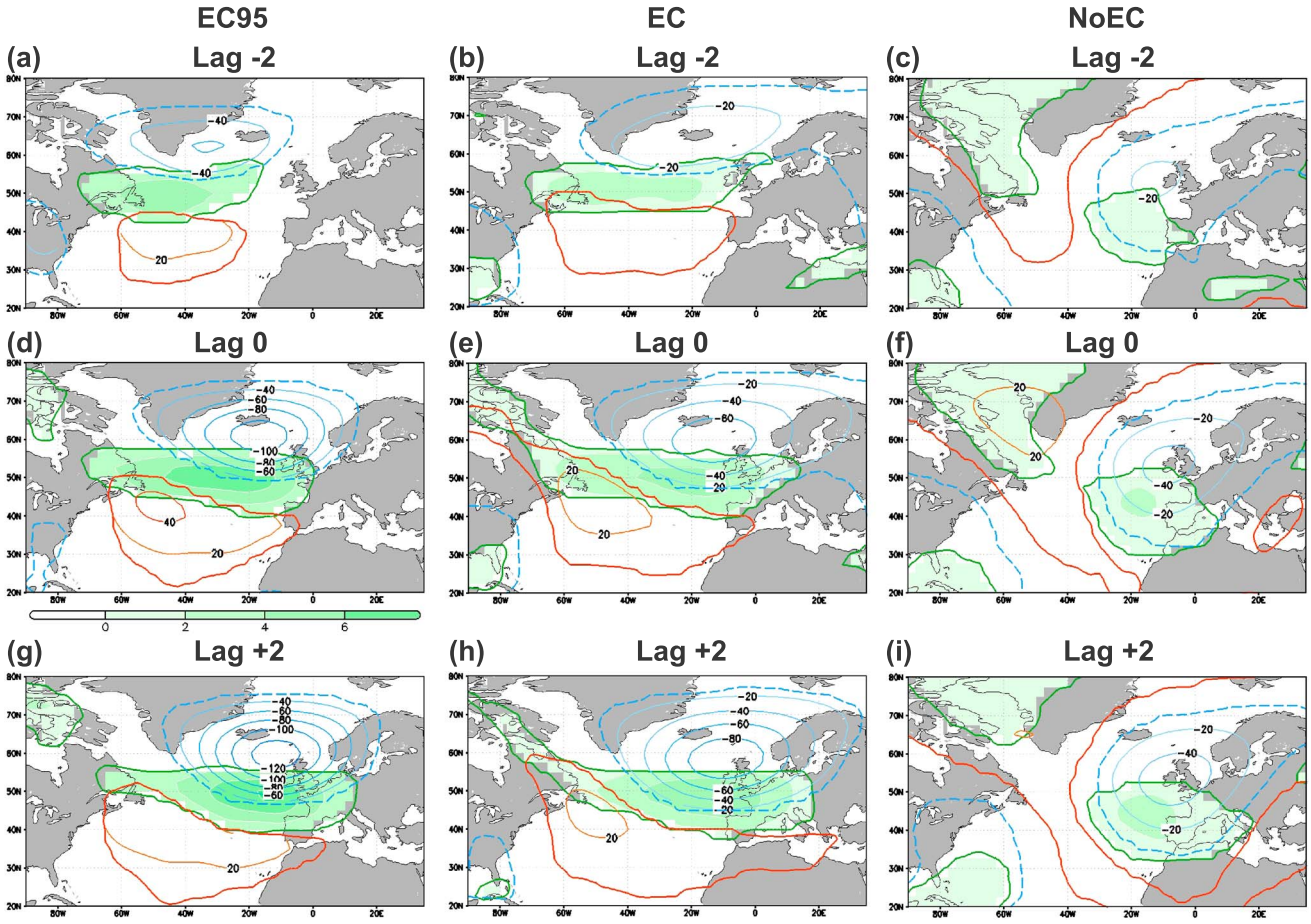

Figure 2. (a)–(i) Composites: significant positive/negative daily z500 anomalies (in gpm at lags −2, 0, and +2, red/blue contours) of (left column) EC95, (central column) EC, and (right column) NoEC. Significant positive 250 hPa jet intensity anomalies in green shadings ($m\,s^{-1}$). Confidence interval: 99%—Monte Carlo test. A 5 day running mean smoothing is applied to the daily anomalies of all variables.

over Western Europe at lag 0 (Figure 2d). This configuration may be forced by RWB at negative lags, which leads to the intensification of the jet stream [*Hanley and Caballero*, 2012; *Gómara et al.*, 2013]. As a consequence, cyclones encounter very favorable upper-level conditions for explosive growth [*Uccellini*, 1990].

Conversely, NoEC predominantly develop under a different mean flow pattern (Figures 2c, 2f, and 2i) which is less transient in time. It consists of three centers of action, with negative anomalies over eastern North America and north-western Europe and a positive anomaly over south-western Greenland. Even though the structure does not resemble the NAO pattern, it projects more onto the negative phase due to the high pressure anomalies over Greenland. In this case the mean flow anomalies do not appear to promote rapid intensification as for EC95 but to deflect the cyclone trajectories toward Europe due to the comparatively high pressures near Greenland (Figures 2c and 2f). As expected from their NDR, the anomalies associated with EC (Figures 2b, 2e, and 2h) are a blend of the previous two patterns.

Since the composite analysis includes cyclones spread over a wide area, the broad low in Figure 2 may be affected by the cyclone imprint at 500 hPa, an effect that we aimed to minimize with the 5 day running mean smoothing (compare to the unsmoothed Figure S1). However, the large-scale pattern shown in Figures 2 and S1 does not seem to be an artifact of the analysis: it extends hemispherically (not shown) and displays a similar structure at negative lags, when the cyclones are located far away and much more widespread (positions at lag −2 are shown in Figures S1g, S1h, and S1i).

The previous analysis shows that the background flow associated with explosive and non-explosive cyclones is different. In the following, these differences are quantified using the NAO index.

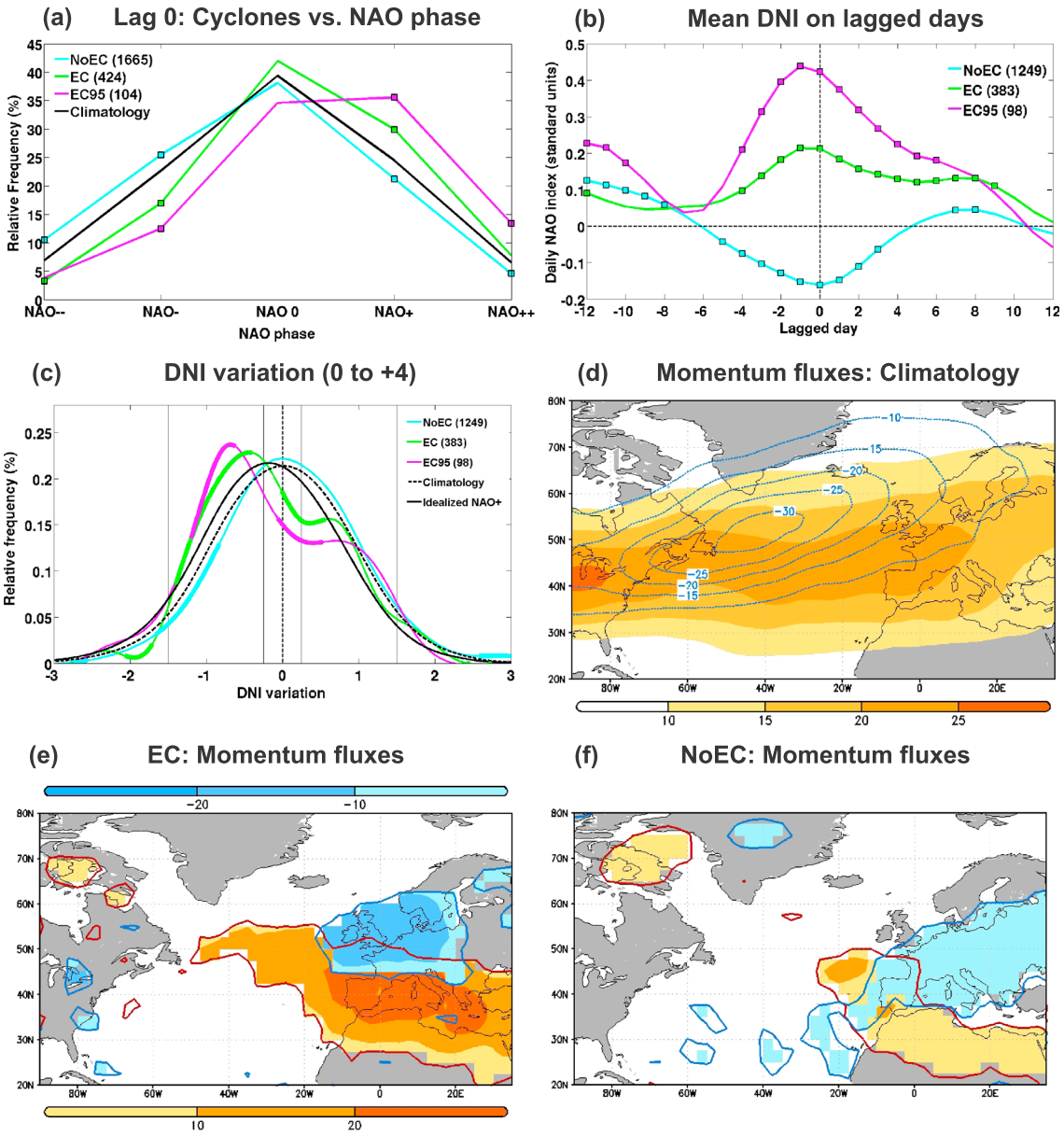

Figure 3. (a) Relative frequency (in % of days) of each NAO phase: climatology (October–March 1950–2010, solid black line); cyclone subsets at lag 0 (NoEC—blue, EC—green, and EC95—magenta). Significant anomalies: black squares. (b) Mean daily NAO index (DNI) (standard units, solid lines) from lags −12 to +12 for cyclone subsets (see legend). Significant anomalies: black squares. (c) Relative frequency (%) of DNI variations ($DNI_{lag+4} - DNI_{lag0}$). Curves: Climatology (dashed black), cyclone subsets (solid blue/green/magenta, see legend). The curves (histograms) are smoothed using a spline interpolation from 0.5 to 0.01 Standard Unit box lengths. Significant anomalies: thicker line. The solid black line is a composite of DNI variations constructed combining climatological distributions for each NAO phase and the frequency of occurrence of that phase for EC95. (d) Climatology of positive (shadings) and negative (contours) high-frequency (1–5 days) Lanczos filtered momentum fluxes over the NA ($m^2 s^{-2}$; daily basis). Positive and negative momentum fluxes are averaged separately (and set to zero when displaying the opposite sign) to avoid compensation. (e) Enhanced positive (red shadings) and negative (blue) momentum fluxes associated with EC (averaged over lags 0 to +4, $m^2 s^{-2}$). (f) Same as Figure 3e but for NoEC. All anomalies are calculated subtracting climatology. Confidence interval: 95%—Monte Carlo test.

3.1.2. Analysis of NAO Conditions

As expected, EC95/EC and NoEC predominantly evolve under different NAO conditions (Figure 3a): whereas a significant shift to negative NAO phases (especially NAO−−) is observed for NoEC compared with climatology, EC95/EC tend to develop under anomalous NAO+.

To provide a more comprehensive view of the NAO behavior, the composite DNI evolution on positive and negative lagged days is shown in Figure 3b. Because of the large lags considered, only cyclones with lag 0

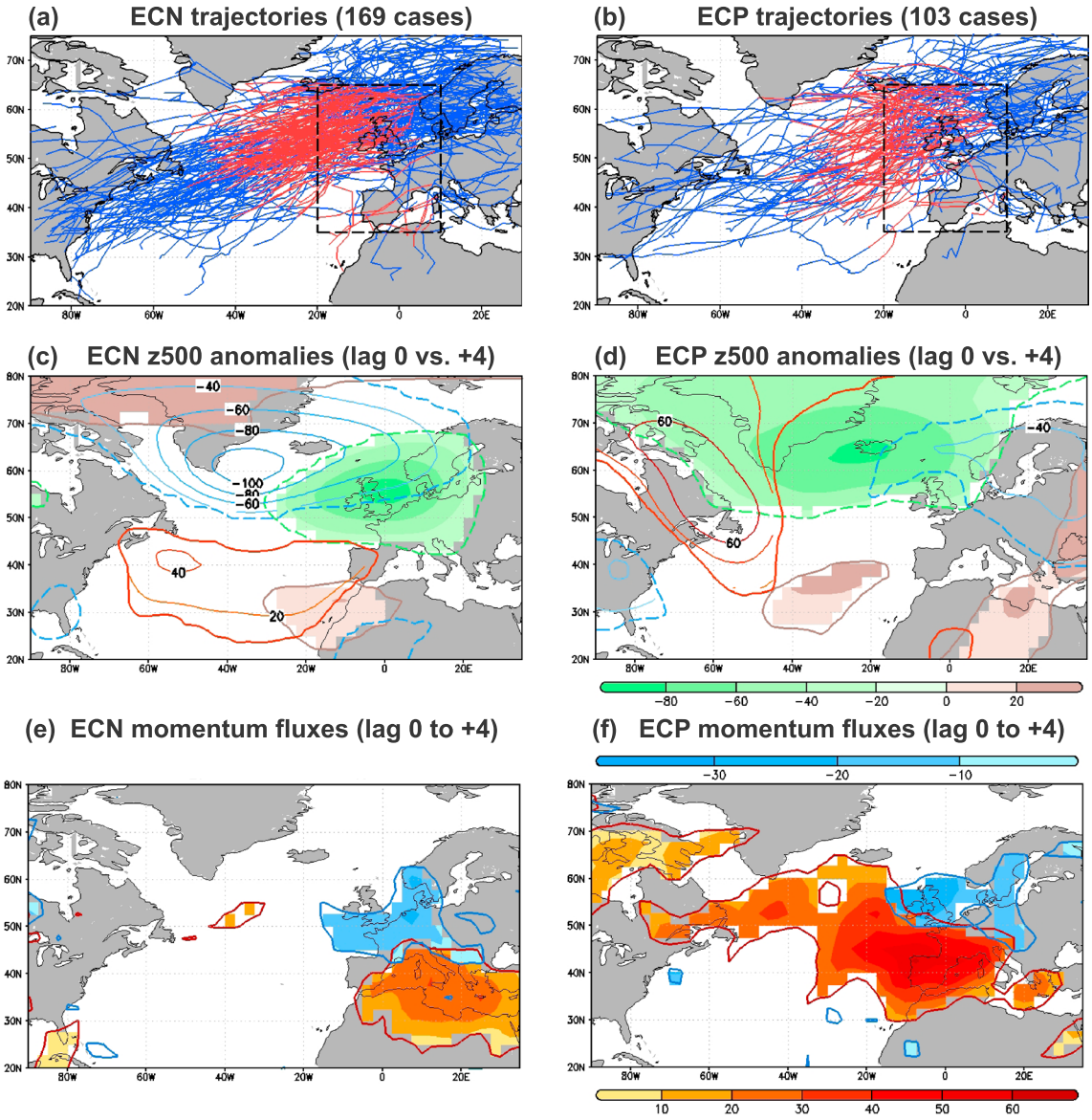

Figure 4. (a) Same as Figure 1a but for Explosive Cyclones followed by Negative NAO variations (ECN). (b) Same as Figure 1a but for Explosive Cyclones followed by Positive NAO variations (ECP). (c) Significant (99%—Monte Carlo test) positive/negative daily z500 anomalies (in gpm, 5 day running means removed) of ECN (red/blue contours—lag 0, grey/green shadings—lag +4). (d) Same as Figure 4c but for ECP. (e) Same as Figure 3e but for ECN. (f) Same as Figure 3e but for ECP.

from 21 October to 10 March are included in this figure. Results suggest that the predominant NAO conditions fostering EC (NoEC) are part of a growing and decaying positive (negative) NAO cycle of 8 to 12 days, peaking around lags −1 to 0 [*Feldstein*, 2003]. Of particular interest is the sharp growth of the DNI index toward positive values for EC95 from lags −6 to −1 (magenta solid line), followed by a decay after peak intensity.

Both the abrupt growth and decay of the DNI for EC95 are consistent with the downstream propagation (and thus higher/lower projection onto the canonical NAO pattern in Figure 1d) of the z500 anomalies. In addition, the growth of this pattern during negative lags might be forced by RWB processes [*Hanley and Caballero*, 2012; *Gómara et al.*, 2013—see their Figure 5] unrelated to the cyclonic development.

3.2. Influence of the Cyclones on the Background Field

In order to investigate the eddy feedback onto the NAO, we analyze the (unsmoothed) DNI variations following the maximum NDR period for the different cyclone samples. Figure 3c shows the relative frequency of DNI variations from lags 0 to +4 ($DNI_{lag+4} - DNI_{lag0}$) for all cyclones in each subset.

Comparison between EC (particularly EC95) and NoEC reveals qualitative differences in the observed distribution of DNI variations after cyclone's peak intensity. For NoEC, the distribution has a Gaussian structure and resembles climatology, except for a small shift to positive values. The latter is consistent with weak frictional damping of the NAO anomalies because this population is characterized by a negative NAO pattern. In contrast, the bimodal distribution of DNI variations for EC/EC95 cannot be explained by frictional effects alone: the idealized NAO+ curve (black solid line in Figure 3c), a composite of DNI variations constructed by combining climatological distributions for each NAO phase and the frequency of occurrence of that phase for EC95, is clearly unimodal. This suggests that other processes like eddy feedbacks [*Lorenz and Hartmann*, 2001] might also play a role in this case.

In order to understand the differences between EC and NoEC, we calculate the high-frequency eddy momentum fluxes (EMF) associated with both subsets (2).

$$EMF = u'v', \tag{2}$$

where u' and v' represent high-frequency (1–5 days) Lanczos filtered zonal and meridional winds at 250 hPa. Climatological values over the NA are shown in Figure 3d. Whereas positive momentum fluxes are more zonal and intense over sub-tropical latitudes, negative values tend to deflect poleward along the NA storm track.

Figures 3e and 3f show that while positive eddy momentum fluxes from lags 0 to +4 are enhanced for both EC and NoEC, they are significantly broader and stronger for the former. A more detailed analysis of the eddy momentum fluxes associated with EC95, EC, and NoEC at individual positive lags confirms the high sensitivity of the eddy forcing on cyclone's intensity (see Figure S2). This is consistent with previous case studies [*Rivière and Orlanski*, 2007] and may explain the positive peak in the distribution of DNI variations for EC/EC95 observed in Figure 3c. In contrast, the enhanced negative eddy momentum fluxes appear too far downstream to play a role for the negative DNI variations.

In order to elucidate the dynamics of the DNI variations for EC, two additional subsets are constructed representative of each of the modes in the distribution. For this purpose, explosive cyclones displaying DNI variations (lags 0 to +4) between −1.5/−0.25 and +0.25/+1.5 (thin vertical lines in Figure 3c) are selected. These are named, respectively, "Explosive Cyclones followed by Negative NAO variations" (ECN) and "Explosive Cyclones followed by Positive NAO variations" (ECP). In Figure 4 cyclone trajectories, z500 anomalies (at lags 0 and +4) and anomalous eddy momentum fluxes (integrated from lags 0 to +4) associated with ECN and ECP are provided. The first clear difference is that cyclone trajectories are tighter for the former, which may have dynamical implications as discussed below.

ECN z500 anomalies are characterized by a downstream propagating NAO+ structure (Figure 4c), similar to the composite pattern for EC95 (Figures 2a, 2d, and 2g). That pattern is also associated with a strong zonal jet, which may account for the explosive intensification. As lags progress, the whole pattern shifts southeastwardly (Figure 4c), and the projection onto the canonical NAO (Figure 1d) is reduced. Since the anomalous eddy momentum fluxes are weak and predominantly positive (Figure 4e), downstream propagation must be the dominant mechanism for the negative DNI variations in this subset.

On the other hand, the ECP z500 anomaly at lag 0 (Figure 4d) resembles the pattern found for NoEC (Figure 2f), which seems to deflect cyclones toward Europe. Since the jet stream is weaker in this case, the explosive intensification of ECP might be primarily influenced by low-level processes [e.g., moist adiabatic processes; *Fink et al.*, 2012; *Dacre and Gray*, 2013] instead of upper-level forcing. On positive lags, positive eddy momentum fluxes are strong and extensive (Figure 4f), which likely explains the positive DNI variations for this subset.

4. Concluding Remarks

In this study the two-way relationship between the North Atlantic Oscillation (NAO) and cyclones affecting Europe is systematically analyzed using reanalysis data. For this purpose, cyclones are classified into three different subsets depending on their intensity, and the NAO is divided into five different classes using a daily index (DNI). We have focused on contrasting explosive vs. non-explosive cyclones, an aspect not analyzed in previous studies.

Composite analysis shows that explosive (EC/EC95) and non-explosive cyclones (NoEC) tend to develop (lags −4 to 0) under different mean flow (and therefore NAO) conditions. On one hand, EC95 (5% most intense cyclones) evolve under a positive NAO-like pattern (Figures 2a, 2d, and 2g), associated with an intensified jet stream over Western Europe. This upper-level configuration is known to foster explosive growth of cyclones [*Uccellini*, 1990; *Hanley and Caballero*, 2012; *Gómara et al.*, 2013]. On the other hand, NoEC are linked to a tripole pattern (wave-like, arched in the NA) of z500 anomalies (Figures 2c, 2f, and 2i). Although this second pattern does not resemble the canonical NAO structure, it projects more onto NAO− due to a common center of action near Greenland (by construction of the index) and is similar to the Greenland Anticyclone pattern described by *Vautard* [1990]. Dynamically, it appears to deflect cyclone's trajectories toward Europe. The spatial extent and temporal evolution of the observed anomalies suggest that they reflect real large-scale circulation patterns and not just the cyclone's imprint (Figures 2 and S1).

After cyclone's peak intensity (lags 0 to +4), contrasting NAO behavior is observed for explosive and non-explosive cyclones. Not surprisingly, explosive cyclones tend to produce stronger DNI variations, both positive and negative, although for different reasons in each case. Negative DNI variations are due to the downstream (both eastward and equatorward) propagation of the z500/jet structure (NAO+ like) and are observed for a large number (169/424) of EC. This propagation results in a reduced projection onto the canonical NAO pattern as lags progress (compare Figures 1d and 4c). Positive DNI variations are due to enhanced positive eddy momentum fluxes, which appear to force a NAO+ on positive lags (compare z500 anomalies at lags 0 and +4 in Figure 4d). This is observed in a smaller subset (103/424) of EC and is typically associated with a weaker jet stream. The enhancement of eddy momentum fluxes with weak upper-level flow and its importance for NAO growth are consistent with previous studies [*Feldstein*, 2003; *Michel and Rivière*, 2011].

The findings from the lag composite analysis performed in this study may contribute to improve predictions (lags −4/−3) of cyclones impacting Europe and enhance the predictability on short-term NAO-like variability. Topics for future research include cyclone clustering during the reported NAO+ episodes and the impact of lower frequency variability (e.g., interannual, multidecadal etc.) over eastern North Atlantic cyclones.

Acknowledgments

We are indebted to the National Centers for Environmental Prediction (NCEP) and NOAA Climate prediction Center for the reanalysis and daily NAO index data. This work was supported by Spanish national funds: research projects MULCLIVAR (CGL2012-38923-C02-01) and DEVIAJE (CGL2009-06944). J. G. Pinto was partially supported by the German Federal Ministry of Education and Research (BMBF) under the project "Probabilistic Decadal Forecast for Central and western Europe" (MIKLIP-PRODEF, contract 01LP1120A). We thank Carlos Yagüe (UCM), Concepción Rodríguez-Puebla (USAL), Javier García-Serrano (LOCEAN/IPSL), and Jorge López-Parages (UCM) for fruitful discussions, and Sven Ulbrich (Univ. Cologne) for help with cyclone data. We also thank the two anonymous reviewers for their helpful comments and suggestions, which contributed to improve this manuscript.

The Editor thanks two anonymous reviewers for assistance in evaluating this manuscript.

References

Dacre, H. F., and S. L. Gray (2013), Quantifying the climatological relationship between extratropical cyclone intensity and atmospheric precursors, *Geophys. Res. Lett.*, *40*, 2322–2327, doi:10.1002/grl.50105.

Donat, M. G., G. C. Leckebusch, J. G. Pinto, and U. Ulbrich (2010), Examination of wind storms over Central Europe with respect to circulation weather types and NAO phases, *Int. J. Climatol.*, *30*, 1289–1300.

Feldstein, S. B. (2003), The dynamics of NAO teleconnection pattern growth and decay, *Q. J. R. Meteorol. Soc.*, *129*, 901–924.

Fink, A. H., T. Brücher, V. Ermert, A. Krüger, and J. G. Pinto (2009), The European storm Kyrill in January 2007: Synoptic evolution and considerations with respect to climate change, *Nat. Hazards Earth Syst. Sci.*, *9*, 405–423.

Fink, A. H., S. Pohle, J. G. Pinto, and P. Knippertz (2012), Diagnosing the influence of diabatic processes on the explosive deepening of extratropical cyclones, *Geophys. Res. Lett.*, *39*, L07803, doi:10.1029/2012GL051025.

Gómara, I., J. G. Pinto, T. Woollings, G. Masato, P. Zurita-Gotor, and B. Rodríguez-Fonseca (2013), Rossby wave-breaking analysis of explosive cyclones in the Euro-Atlantic sector, *Q. J. R. Meteorol. Soc.*, doi:10.1002/qj.2190.

Hanley, J., and R. Caballero (2012), The role of large-scale atmospheric flow and Rossby wave breaking in the evolution of extreme windstorms over Europe, *Geophys. Res. Lett.*, *39*, L21708, doi:10.1029/2012GL053408.

Hurrell, J. W., Y. Kushnir, G. Ottersen, and M. Visbeck (2003), An overview of the North Atlantic Oscillation, in *The North Atlantic Oscillation: Climate Significance and Environmental Impact*, *Geophys. Monogr. Ser.*, vol. 134, edited by J. W. Hurrell, pp. 279, AGU, Washington, D. C.

Kalnay, E., et al. (1996), The NCEP/NCAR 40-year reanalysis project, *Bull. Am. Meteorol. Soc.*, *77*, 437–471.

Lamb, H. H. (1991), *Historic Storms of the North Sea, British Isles, and Northwest Europe*, pp. 204, Cambridge Univ. Press, Cambridge, U. K., and New York.

Lorenz, D., and D. Hartmann (2001), Eddy-zonal flow feedback in the Southern Hemisphere, *J. Atmos. Sci.*, *58*, 3312–3327.

Michel, C., and G. Rivière (2011), The link between Rossby wave breakings and weather regime transitions, *J. Atmos. Sci.*, *68*, 1730–1748, doi:10.1175/2011JAS3635.1.

Michel, C., G. Rivière, L. Terray, and B. Joly (2012), The dynamical link between surface cyclones, upper-tropospheric Rossby wave breaking and the life cycle of the Scandinavian blocking, *Geophys. Res. Lett.*, *39*, L10806, doi:10.1029/2012GL051682.

Murray, R. J., and I. Simmonds (1991), A numerical scheme for tracking cyclone centers from digital data. Part I: Development and operation of the scheme, *Aust. Meteorol. Mag.*, *39*, 155–166.

Pinto, J. G., and C. C. Raible (2012), Past and recent changes in the North Atlantic oscillation, *WIREs Clim. Change*, *3*, 79–90, doi:10.1002/wcc.150.

Pinto, J. G., T. Spangehl, U. Ulbrich, and P. Speth (2005), Sensitivities of cyclone detection and tracking algorithm: Individual tracks and climatology, *Meteorol. Z.*, *14*, 823–838.

Pinto, J. G., S. Zacharias, A. H. Fink, G. C. Leckebusch, and U. Ulbrich (2009), Factors contributing to the development of extreme North Atlantic cyclones and their relationship with the NAO, *Clim. Dyn.*, *32*, 711–737.

Raible, C. C. (2007), On the relation between extremes of midlatitude cyclones and the atmospheric circulation using ERA40, *Geophys. Res. Lett.*, *34*, L07703, doi:10.1029/2006GL029084.

Rivière, G., and I. Orlanski (2007), Characteristics of the Atlantic storm-track eddy activity and its relation with the North Atlantic Oscillation, *J. Atmos. Sci.*, *64*, 241–266.

Sanders, F., and J. R. Gyakum (1980), Synoptic-dynamic climatology of the bomb, *Mon. Weather Rev.*, *108*, 1589–1606.

Uccellini, L. W. (1990), Processes contributing to the rapid development of extratropical cyclones, in *Extratropical Cyclones - The Erik Palmen Memorial Volume*, edited by C. Newton and E. O. Holopainen, pp. 81–105, Am. Meteorol. Soc, Boston, Mass.

Vautard, R. (1990), Multiple weather regimes over the North Atlantic: Analysis of precursors and successors, *Mon. Weather Rev.*, *118*, 2056–2081.

Wernli, H., S. Dirren, M. A. Liniger, and M. Zillig (2002), Dynamical aspects of the life-cycle of the winter storm "Lothar" (24–26 December 1999), *Q. J. R. Meteorol. Soc.*, *128*, 405–429.